Uranium-series geochronology of travertine from Soda Dam, New Mexico: A Quaternary record of episodic spring discharge and river incision in the Jemez Mountains

April Jean, Laura J. Crossey, Karl E. Karlstrom, Victor J. Polyak, and Yemane Asmerom, [eds.]
2024, pp. 257-270. https://doi.org/10.56577/FFC-74.257
Supplemental data: https://nmgs.nmt.edu/repository/index.cfml?rid=2024004

in:

Geology of the Nacimiento Mountains and Rio Puerco Valley, Karlstrom, Karl E.;Koning, Daniel J.;Lucas, Spencer G.;Iverson, Nels A.;Crumpler, Larry S.;Aubele, Jayne C.;Blake, Johanna M.;Goff, Fraser;Kelley, Shari A., New Mexico Geological Society 74 th Annual Fall Field Conference Guidebook, 334 p.

This page is intentionally left blank to maintain order of facing pages.

New Mexico Geological Society Guidebook, 74th Fall Field Conference, 2024, p. 257–270, https://doi.org/10.56577/FFC-74.257

URANIUM-SERIES GEOCHRONOLOGY OF TRAVERTINE FROM SODA DAM, NEW MEXICO: A QUATERNARY RECORD OF EPISODIC SPRING DISCHARGE AND RIVER INCISION IN THE JEMEZ MOUNTAINS

APRIL JEAN[1], LAURA J. CROSSEY[1], KARL E. KARLSTROM[1], VICTOR J. POLYAK[1], AND YEMANE ASMEROM[1]

[1]Department of Earth and Planetary Sciences, Northrop Hall, 221 Yale Blvd. NE, University of New Mexico, Albuquerque, New Mexico 87131; kek1@unm.edu

Abstract—This paper uses the extraordinary field laboratory of Soda Dam, an iconic travertine deposit in New Mexico, to analyze the history of interactions of magmatism, paleohydrology, and tectonics in the Jemez Mountains hydrothermal system. We dated 37 samples via uranium-series (U-series) geochronology to constrain the timing of travertine deposition at Soda Dam. Travertine U-series dates (n = 35) and $\delta^{234}U$ model ages (n = 2) range from 755±212 ka to 2.14±0.03 ka. These data demonstrate that the hydrothermal system has been episodically active over the past ~1 million years with main episodes around 500, 210, 120, and <10 ka. Age modes do not correlate well with glacial-interglacial periods or with periods of volcanism. Younger infillings within older travertine deposits, including in the highest accumulation, suggest that travertine deposition was linked to periods of high head in the Valles Caldera recharge region for the Jemez River and artesian fault conduits. These episodes may record intervals when major caldera lakes occupied the Valles caldera at ~500 ka, during the climatic transition from MIS 6 to 5 (~120 ka), during MIS 5C (~100 ka), and at the beginning of the Holocene.

INTRODUCTION

The travertine-depositing hot springs at Soda Dam, New Mexico, provide an unparalleled field laboratory that preserves a datable record of the interactions between the dormant Quaternary Valles Caldera supervolcano system, high-elevation caldera lakes, a single river outflow, and a groundwater system involving mixed geothermal and meteoric waters. This system records marked paleohydrologic changes that occurred while the Jemez River incised San Diego Canyon following the last major ignimbrite eruption of the Valles Caldera 1.23 million years ago. The ability to link modern processes to a long-lived travertine record is helpful for understanding the interactions among tectonic, magmatic, and climatic processes that shape landscapes and influence groundwater quality. Soda Dam itself is a vein-fed fissure ridge that has intermittently and partially dammed the Jemez River (Fig. 1). Previous work has suggested that travertine deposition in the arid Southwest may be episodic and associated with wet conditions (Szabo, 1990; Asmerom et al., 2006; Crossey et al., 2006; Embid, 2009; Priewisch et al., 2013). Ancient travertine deposits positioned high in the landscape are resistant to weathering in arid climates and can preserve fragments of past landscapes. In incising landscapes, travertine can cement and thus record changing base level and associated incision rates in southwestern river systems (Pederson et al., 2006; Karlstrom et al., 2008). In situations of long-lived spring-fed travertine platforms and inverted topography, the presence of younger travertine infillings within older accumulations can provide insight into past hydrologic conditions, including fluctuation in the elevation of local hydrologic head through time (Priewisch et al., 2013). Thus, U-series dating of

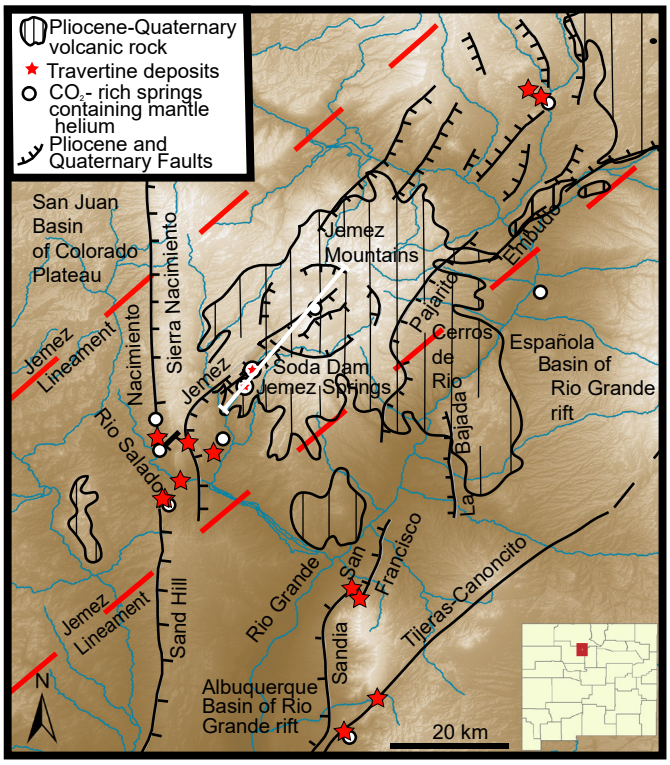

FIGURE 1. Index map (DEM) of the Jemez Mountain region of northern New Mexico. Lighter colors are higher-elevation regions. The Jemez Mountains and Valles Caldera are located at the intersection of the Rio Grande rift and Jemez lineament. Neotectonic features of this area include Quaternary extensional and transtensional faults, Plio-Pleistocene volcanic fields (line pattern), carbonic springs with mantle ^3He and high CO_2 (white dots), and Quaternary travertine deposits (stars). The cross-section line for Figure 2 is shown in white.

geologically well-constrained travertine occurrences has rich potential for constraining past paleohydrology and paleolandscape evolution.

The Soda Dam study area is located along the Jemez fault zone where it crosses the Jemez River of San Diego Canyon, the main perennial discharge from the Jemez Mountains. The Valles Caldera, headwaters of the Jemez River, was the center of massive rhyolite ash-flow tuff eruptions at 1.62 and 1.23 Ma (dates from Nasholds and Zimmerer, 2022). Hence its travertine record may provide insight into the interplay of magmatism, faulting, climate, and groundwater. The modern Jemez Mountains hydrothermal system overlies a shallow magma system at 3–10 km depth near the center of the caldera that may contain melt fractions up to ~20% (Wilgus et al., 2023, and references therein). Outflow of geothermal waters follows the Jemez fault system to the southwest in a fault-influenced set of flow paths subparallel to the Jemez River in San Diego Canyon. The hydrothermal system is recharged by meteoric water that infiltrates primarily within the high elevation (>3 km) watersheds of the Valles Caldera. A fault-parallel cross section (Fig. 2; Goff, 2009) postulates that geothermal waters mix with meteoric waters along the various strands of the Jemez fault zone that include the Soda Dam fault, feeding a series of hot and warm springs. The Jemez River, springs, and groundwater aquifers have variable hydrochemistry that indicate complex mixing between different water sources (Goff and Janik, 2002; McGibbon et al., 2018).

The goals of this paper are to provide descriptions, accumulation volumes, and U-series dates for the travertine deposits of the Soda Dam system. We also provide a more detailed map using recent work of Moats (2004) and Kelley et al. (2003) and additional field mapping to refine locations of travertine deposition and their relationship to faults and river terraces. Jean (2012) evaluated conditions of modern and past travertine deposition using stable isotopes of carbon and oxygen measured in travertine, modern water, and $CO_{2(gas)}$, but those data are not reported here and are beyond the scope of this paper.

TRAVERTINE FORMATION AND CO_2 ORIGINS

The term travertine is used here in the broad sense to include freshwater carbonate deposits that precipitate through degassing of carbon dioxide (CO_2) from a groundwater source, leading to calcium carbonate supersaturation and carbonate precipitation in a variety of depositional environments (Pentecost, 2005). Travertine deposition involves acquisition of solutes in groundwater from the host rock through dissolution due to excess CO_2 (carbonic acid, H_2CO_3, when dissolved), aqueous transport of the dissolved solutes through the aquifer system, and deposition of travertine (usually as calcite, $CaCO_3$) at a discharge location (Crossey et al., 2009).

Hydrothermal waters (~47°C) that are associated with volu-

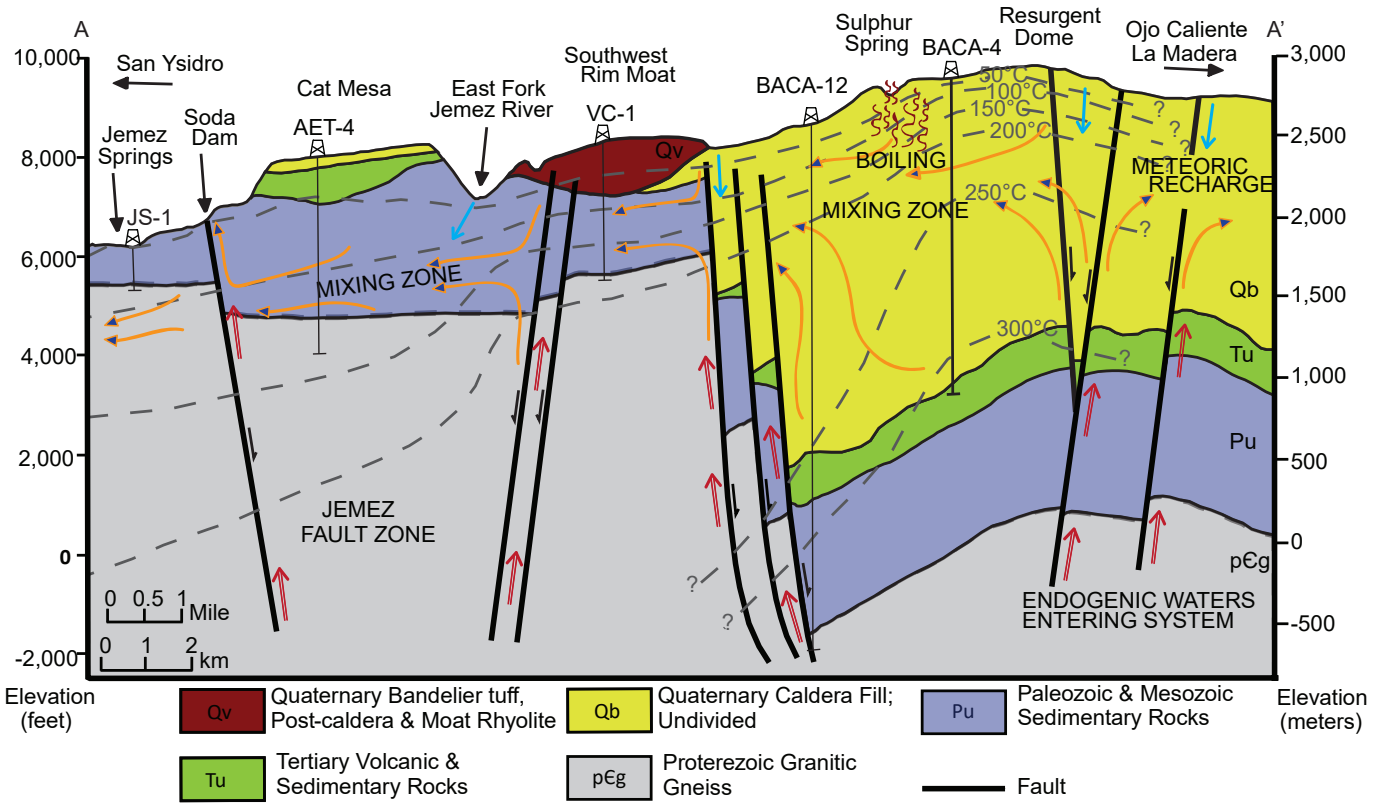

FIGURE 2. Fault-parallel northeast-southwest cross section of the Jemez Mountains hydrothermal system from Valles Caldera to Jemez Springs (modified from Goff, 2009; see Fig. 1 for location). Red arrows depict endogenic waters moving upward along faults and mixing (orange arrows) with meteoric waters (blue arrows) in Paleozoic aquifer units and fractured basement. Dashed lines are isotherms. Flow of the hydrothermal plume down San Diego Canyon parallels the surface flow and follows the complex Jemez fault zone. Soda Dam and Jemez Springs are windows where supersaturated carbonic waters that contain mantle ^3He ascend to the surface, degas CO_2, and precipitate travertine. Locations and depths of wells are from Goff (2009).

minous travertine deposition at Soda Dam are highly charged with CO_2 and have amassed a large dissolved calcite load, which partially neutralizes acidic pH and increases the concentrations of calcium and magnesium and the alkalinity of the groundwater (Crossey et al., 2006, 2009). When these waters emerge at the spring vent, they are exposed to the lower P_{CO2} of the atmosphere, causing CO_2 degassing and travertine precipitation.

High $^3He/^4He$ ratios in many travertine-depositing springs and groundwaters of the Jemez Mountains indicate the presence of volatiles that were derived in part from the mantle (Goff and Janik, 2002; Newell et al., 2005; Crossey et al., 2011). $^3He/^4He$ ratios measured in deep geothermal wells (Baca wells) are as high as 5.72 R_A, and Sulphur Springs ratios in the Valles Caldera reach up to 6.16 R_A (Goff and Janik, 2002), where R_A = air $^3He/^4He = 1.384 \times 10^{-6}$. Average mid-ocean ridge basalt (MORB) values are ~8 R_A. Thus, at Sulphur Springs, about 75% of the total helium is derived from the mantle. CO_2, the carrier gas for the helium, is also mainly of mantle origin (Ballentine and Burnard, 2002; Ballentine et al., 2002; Crossey et al., 2011). Mixing occurs between hydrothermal waters and meteoric waters, and consequently Soda Dam spring waters have lower $^3He/^4He$ of 0.84±0.05 R_A (Goff and Janik, 2002) than the deep geothermal wells or inner caldera springs. This value suggests about 10% of the helium at Soda Dam is of mantle origin.

GEOLOGIC AND HYDROLOGIC SETTING OF THE SODA DAM SYSTEM

Soda Dam is a popular tourist attraction with cultural significance for local Native American communities. The travertine deposits are situated along the Jemez River, which cuts through the Jemez Mountains from the caldera rim, down the southwestern flank of the Jemez Mountains volcanic field, and eventually drains into the Rio Grande. The Jemez Mountains volcanic field contains an array of basaltic through rhyolitic rocks but is most widely recognized for the massive caldera-forming supervolcano eruption events that took place 1.62 and 1.23 Ma (Nasholds and Zimmerer, 2022) creating the Toledo and Valles Calderas, respectively, and producing ~2,000 km^3 of erupted material (Goff, 2009).

The Jemez Mountains lie along the tectonically and magmatically active Jemez lineament and straddle the boundary between the Colorado Plateau and the Rio Grande rift. The Soda Dam travertine deposits are located 3 km southwest of and 1000 m down-elevation-gradient from the Valles Caldera, where the Jemez fault zone crosses the Jemez River. This fault zone acts as a subsurface conduit within several permeable Paleozoic aquifer units and fractured basement, channeling hydrothermal and meteoric waters through San Diego Canyon. The Soda Dam fault, one strand of the Jemez fault zone, was initially a southeast-side-up Laramide reverse fault and is parallel to the steeply dipping limb of a monoclinal bend in the Paleozoic strata (Fig. 3). This and adjacent strands have been reactivated as normal faults and offset Pennsylvanian-Permian rocks by 200–250 m and the upper Bandelier Tuff 15 m west of Soda Dam (Kelley et al., 2003).

The high-elevation caldera watershed has varied over time, from grasslands with shallow groundwater to marshes and caldera lakes, depending on seasonality and climate shifts. San Diego Canyon has served as a drainage outlet for the headwaters that form within the Valles Caldera since the Pliocene, when the paleocanyon's axis was positioned west of the modern canyon (Kelley et al., 2003). The paleocanyon was filled with 1.85 Ma La Cueva Member of the Bandelier Tuff, but continued to incise on the western paleoaxis, as indicated by gravel deposits between the La Cueva and Otowi Members of the Bandelier Tuff, which capped the 1.62 Ma landscape (Kelley et al., 2003; Goff, 2009). River gravels are preserved in several locations between the lower Otowi and upper Tshirege Members of the Bandelier Tuff (Kelley et al., 2003). Parts of the post–1.23 Ma reincision history of San Diego Canyon is recorded by travertine deposits at Soda Dam.

Caldera lakes have occupied the Valles Caldera numerous times since the eruption of the upper Bandelier Tuff. The first paleolake occupied the caldera just following the 1.23 Ma eruption and likely drained due to the resurgent dome rising at a rate of 0.1 ft/yr for 30 ka (Goff, 2009; Fawcett et al., 2011). Subsequent small rhyolitic eruptions blocked surface drainage, forming lakes around 0.8 Ma (Goff, 2009; Fawcett et al., 2011). The San Antonio and South Mountain dome rhyolitic eruptions dammed the Jemez River, forming a relatively persistent lake in the Valle Grande for at least 189 ka, from 520 ka to approximately 360 ka, as documented from an 82-m lacustrine sediment core (VC-3; Fawcett et al., 2011). The last eruption series in the Jemez Mountains was the Battleship Rock Tuff and El Cajete Pumice beds at 74 ka, followed by eruption of the Banco Bonito lava flow at about 68 ka. El Cajete Pumice blocked the East Fork of the Jemez River and formed a short-lived lake in the Valles Caldera (Goff, 2009).

A large groundwater reservoir in the modern Valles Caldera occurs in the subsurface caldera-fill tuff and associated sedimentary rocks (Goff and Gardner, 1994). Stable isotope analysis of streams and groundwaters reveals δD values that are consistent with meteoric recharge within the Valles Caldera (Heinken et al., 1990). Meteoric recharge infiltrates to depths of approximately 2–3 km, where it is heated to temperatures >300°C and mixes with CO_2-rich endogenic fluids that rise within the complex fault system (Fig. 2; Heinken et al., 1990; Goff, 2002). The thermal waters are convected to approximately 500–600 m in depth before migrating downgradient through the Jemez fault zone and local aquifer units (Heinken et al., 1990).

Deep reservoir fluids that have been encountered by the Baca wells in Redondo Creek Graben and similar waters reach the surface naturally at Sulphur Springs (Fig. 2). These endogenic waters are similar with respect to ratios of conservative tracers (B/Cl, Br/Cl, and Li/Cl) to the fluids discharged by hot springs at the Soda Dam location (Goff and Gardner, 1994). These are neutral pH-chloride waters with total dissolved solids (TDS) averaging 7,000 mg/L; concentrations of Na + K exceeding Ca + Mg; high concentrations of SiO_2; and high As, B, Br, Cs, Li, and Rd concentrations (Goff and Gardner, 1994).

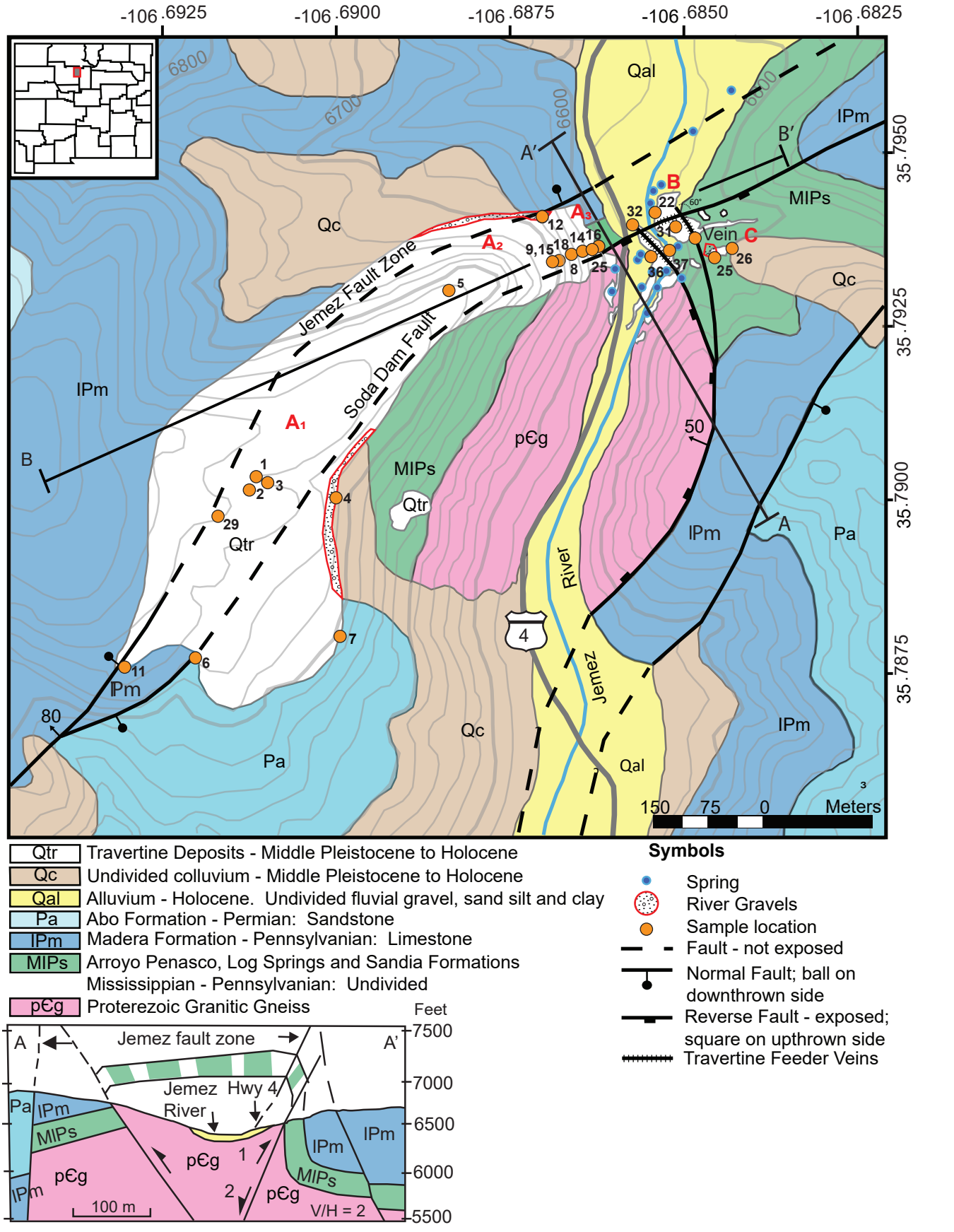

FIGURE 3. Geologic map of the Soda Dam study area (modified from Goff and Shevenell, 1987; Kelley et al., 2003; and Moats, 2004) depicting locations of the main travertine deposits, active springs, and major faults that act as fluid conduits. Sample numbers correspond to Table 1. Location of the B-B' cross-canyon profile of Figure 8 is shown. The A-A' cross section shows Laramide reverse faults reactivated by Quaternary extension.

Water from wells and inner caldera springs have relatively positive $\delta^{18}O$ values of -8.41 to -9.96‰ (Vuataz and Goff, 1986; Goff and Janik, 2002), which are characteristic of hydrothermal systems.

The Soda Dam area contains approximately 20 active thermal and nonthermal springs and seeps that deposit travertine both within and near the banks of the Jemez River (Fig. 3). Temperatures of the springs at Soda Dam are relatively constant; the main hot spring on the west side of the highway emerges at approximately 47°C and the "Grotto" spring, bubbling up inside Soda Dam itself (Deposit D) emerges at approximately 27°C (Goff and Shevenell, 1987; Jean, 2012). Travertine accumulations are present on both sides of the canyon and extend to elevations >200 m above the river; these high-elevation deposits are not associated with presently active springs or seeps but were deposited around paleospring vents and fissures that were analogous to the modern system (Goff and Shevenell, 1987; Moats, 2004). Thus, all of the travertine outcrops near Soda Dam are considered jointly here under the heading of "Soda Dam travertine." The unique tectonic, hydrogeologic, and geomorphic setting of Soda Dam is such that travertine deposition has interacted with paleohydrology and canyon incision for much of the Quaternary history of San Diego Canyon. Goff and Shevenell (1987) used U-disequilibrium dating to determine that travertine deposition at Soda Dam has been episodic for the past 1.0 Ma, and they recognized four main deposits: (1) Deposit A is the high platform developed on the western side of San Diego Canyon. (2) Deposits B and C are inactive fissure-ridge and mound travertine deposited on the eastern banks of the Jemez River. (3) Deposit D is the Soda Dam. Carbonate dating by Goff and Shevenell (1987) took place at an earlier stage in the development of U-series dating and used an alpha counting technique that is less precise and less accurate than the current methods discussed in this paper, which used mass spectrometry. Despite the improvement of techniques through time, the relative ages of the deposits established by Goff and Shevenell (1987) served as a useful framework for this study.

METHODOLOGY

Subsamples selected for U-series geochronology were drilled powders that were dissolved in 15N nitric acid and spiked with a mixed solution containing known concentrations of ^{229}Th, ^{233}U, and ^{236}U. Procedural blanks are between 5 and 30 pg for both ^{232}Th and ^{238}U. All laboratory work was completed in the Radiogenic Isotope Laboratory at the University of New Mexico using a Thermo Neptune multicollector inductively coupled plasma mass spectrometer following the standard procedures of Asmerom et al. (2006) and using the decay constants of Cheng et al. (2013). For samples outside of U-series dating range, we calculated $\delta^{234}U$ model ages, assuming a δ^{234}_{i} value that is the average of the range of the 15 samples with measured δ^{234}_{i} values from the older Deposit A (605‰ ± 50%). See details in Appendix 1.

MAPPING RESULTS: TRAVERTINE DISTRIBUTION, LANDSCAPE POSITION, AND VOLUMES

Figure 3 shows the locations and extent of the four major travertine deposits. The deposits are described below and ages are listed in Table 1 from oldest to youngest. Deposit A1 (Fig. 4A) forms a platform accumulation west of the river that overlies river gravels at its base (at 2060 m; Fig. 4B) and extends to an elevation 2130 m. It consists of a stratigraphic (micrite) platform intruded by sills and dikes of spar calcite that range from 0.1 to 1 m thick and indicate multiple episodes of infilling deposition (Fig. 4C). This coarse spar calcite is characteristic of precipitation from geothermal waters (Decker et al., 2016), and the horizontal sill geometries with crystals oriented perpendicular to the walls of the horizontal sill indicate the veins opened vertically due to artesian pressure of ascending fluids. No spring vents or fissure ridges have been identified for this platform, and we interpret the deposition to have taken place from springs emanating along strands of the Jemez fault zone when the river bottom was in the position of the exposed gravels, ~0.6 km to the northwest and ~130 m above the modern river position. These springs would have been near river level and broadly analogous to the main active springs that feed Soda Dam today. Deposit A has an average thickness of 20 m and an estimated travertine volume of 2.9×10^6 m^3.

We also identified inset younger deposits on the east side of Deposit A1, which we named A2 and A3. Deposit A2 is identified as the travertine deposits that were draped across east-dipping slopes (e.g., at sample #5) as the river began to incise eastward from the platform toward the present river position. This is similar to deposition occurring at the La Madera travertine deposits along the modern Rio Ojo (Crossey et al., 2011). The micritic drape sequence of Deposits A1 and A2 contain numerous cross-cutting spar calcite veins, which together contain approximately 8.25×10^5 m^3 of travertine. Deposit A3 is a lower and younger inset deposit that accumulated 30 to 65 m above the modern river (Fig. 5), with an average thickness of 20 m and an estimated travertine volume of 3.0×10^5 m^3. This deposit sits on upturned Precambrian and Paleozoic rocks and overlies travertine-cemented river gravels ~30 m above the modern river.

Deposit B (Fig. 6) accumulated on the northeast side of Jemez River along the Soda Dam fault and represents an older analog to the modern fissure ridge/mound system that is building Soda Dam. Maximum elevation is approximately 40 m above the Jemez River. Two central fissures of finely laminated micrite with some spar calcite approximately 1 m wide dissect the deposit. The western fissure trends toward an azimuth of ~070 through the deposit, on trend with the Soda Dam fault. Near the center of the deposit, the second fissure intersects at an azimuth of ~080. Deposit C is a small deposit on the east side of the river that may have been sourced from Deposit B. No evidence of a fissure ridge or extinct spring mounds or vents were found, although sills overlying paleoriver gravels are present at the base (16.5 m above the river). Deposits B and C have a preserved estimated volume of 1.1×10^5 m^3.

Deposit D, the Soda Dam itself, is approximately 100 m

FIGURE 4. View approaching Soda Dam area (below arrow). (A) Deposit A1 is a high travertine platform overlying Paleozoic strata and granite with paleo-Jemez River gravels at its base; A2 drapes down towards the Jemez River, and A3 is inset into A2. (B) Gravels at the base of Deposit A1 show the position of the paleo-Jemez River between ~500 and 700 ka. (C) Sill at base of A1 has vertical spar crystals (dashed lines) that suggest high pore fluid pressure of geothermal waters.

long and 30 m wide with an estimated travertine volume of 2.4 x 10^4 m^3. The deposit sits on a carbonate platform, which has an estimated area of 6,000 m^2 and thickness of up to 1 m. In the past, the main hot spring discharge occurred along a 0.5-m-wide northwest-southeast central fissure system that is aligned with a northwest-striking Laramide reverse fault near where it intersects the northeast-striking Soda Dam strand of the Jemez fault zone. Presently, the main spring discharge occurs along the Soda Dam fault on the west side of State Highway 4 due to damage caused to the plumbing of the structure during highway construction (Goff and Shevenell, 1987). Two small caves on the southeastern side of the Soda Dam structure allow access to the interior of the deposit and indicate that artesian water is still emanating along much of the fissure ridge system. The larger of the two, Grotto spring, consists of a pool approximately 1 m in diameter within a travertine mound covered with a veneer of microterraces. Calcite straws build daily as supersaturated thermal waters drip from the ceiling above

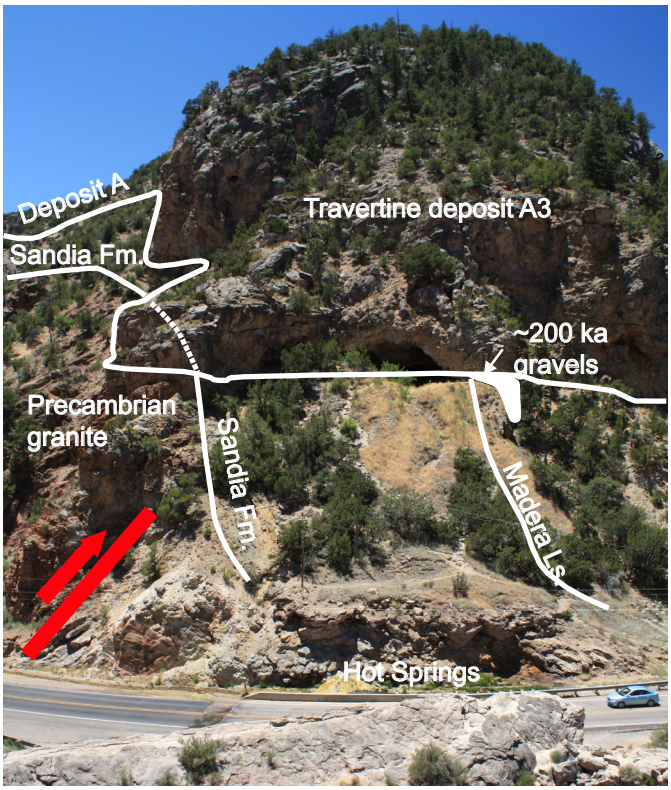

FIGURE 5. View of inset Deposit A3 with Soda Dam and active hot springs in foreground. The cave has ~200 ka paleo-Jemez River gravels atop a strath cut onto the folded Great Unconformity and subvertical basal Paleozoic strata.

the pool. The smaller of the two openings reveals a very small cave at the base of the Soda Dam. Multiple seeps surround the base and platform, many of which deposit travertine. Underneath the mound and platform (accessible from within the river), thermal waters drip directly into the Jemez River in two "lower grottos," depositing calcite straws.

RESULTS OF URANIUM-SERIES GEOCHRONOLOGY

Thirty-seven samples dated from the deposits at Soda Dam are listed from oldest to youngest in Table 1. Figure 3 shows sample locations, and Figure 8 depicts the schematic positions relative to the modern topography and the inferred progressively incising San Diego Canyon paleotopography. Samples were selected to constrain: (1) bottom and top layers (durations) of stratigraphic travertine deposits, (2) samples that cement and were deposited contemporaneously with river gravels in elevated river terraces, (3) spar sills and micrite infillings that crosscut platform deposits and indicate continued discharge within existing platforms, and (4) banded feeder vein systems in Deposits B and D.

At its top, the micritic platform of Deposit A1 was outside of U-series range (>500 ka). However, two micritic samples from near the top of the deposit yielded an imprecise $\delta^{234}U$ model age of 755±212 ka (2 sigma) and an also imprecise U-series age of 560±324 ka. Taken together, we infer that the depositional age for the platform is best approximated by the

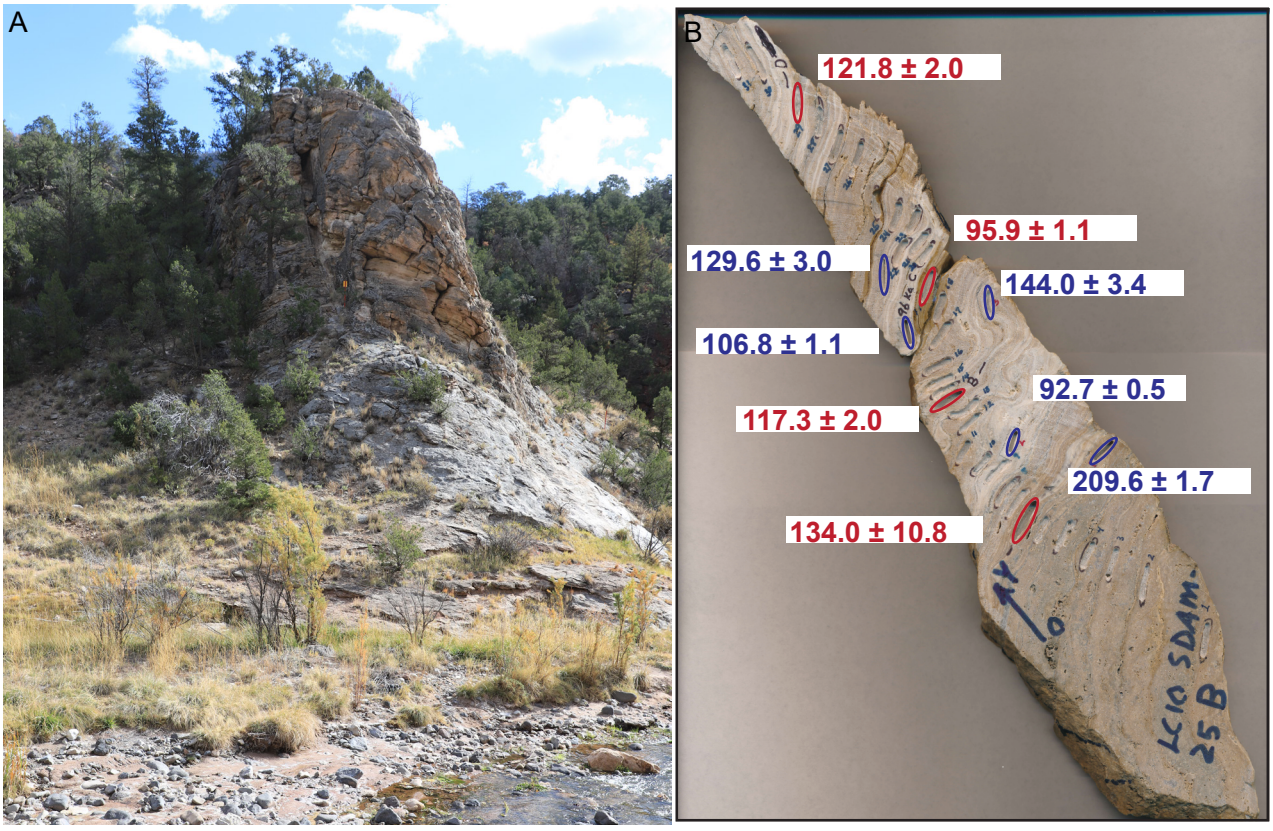

FIGURE 6. Deposit B showing its fissure ridge geometry. Cut slab from Deposit B fissure vein (LC10_SDamB_25) displaying U-series-dated locations. Initial old (O) to young (Y) assumed age progression was disproven, and instead vein growth took place discontinuously and with seemingly random infilling. Duration of vein growth was at least 116.9 ka (from 209.6 to 92.7 ka).

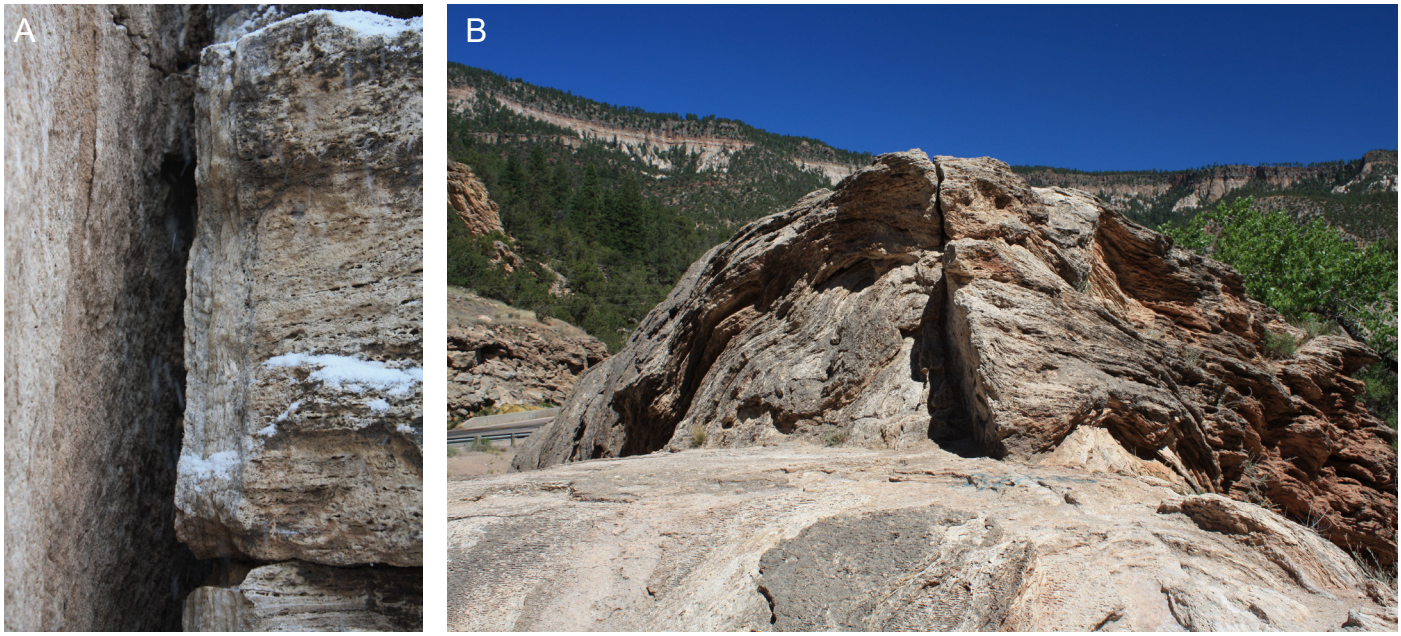

FIGURE 7. Soda Dam (Deposit D). (A) Calcite feeder vein for Soda Dam exposed on road gives ages of 4.6 to 5.2 ka. (B) View looking back toward road from near the southeast end of Soda Dam; the base of the deposit gives an age of 10.0 ka near the road; the top of the deposit gives an age of 2.1 ka.

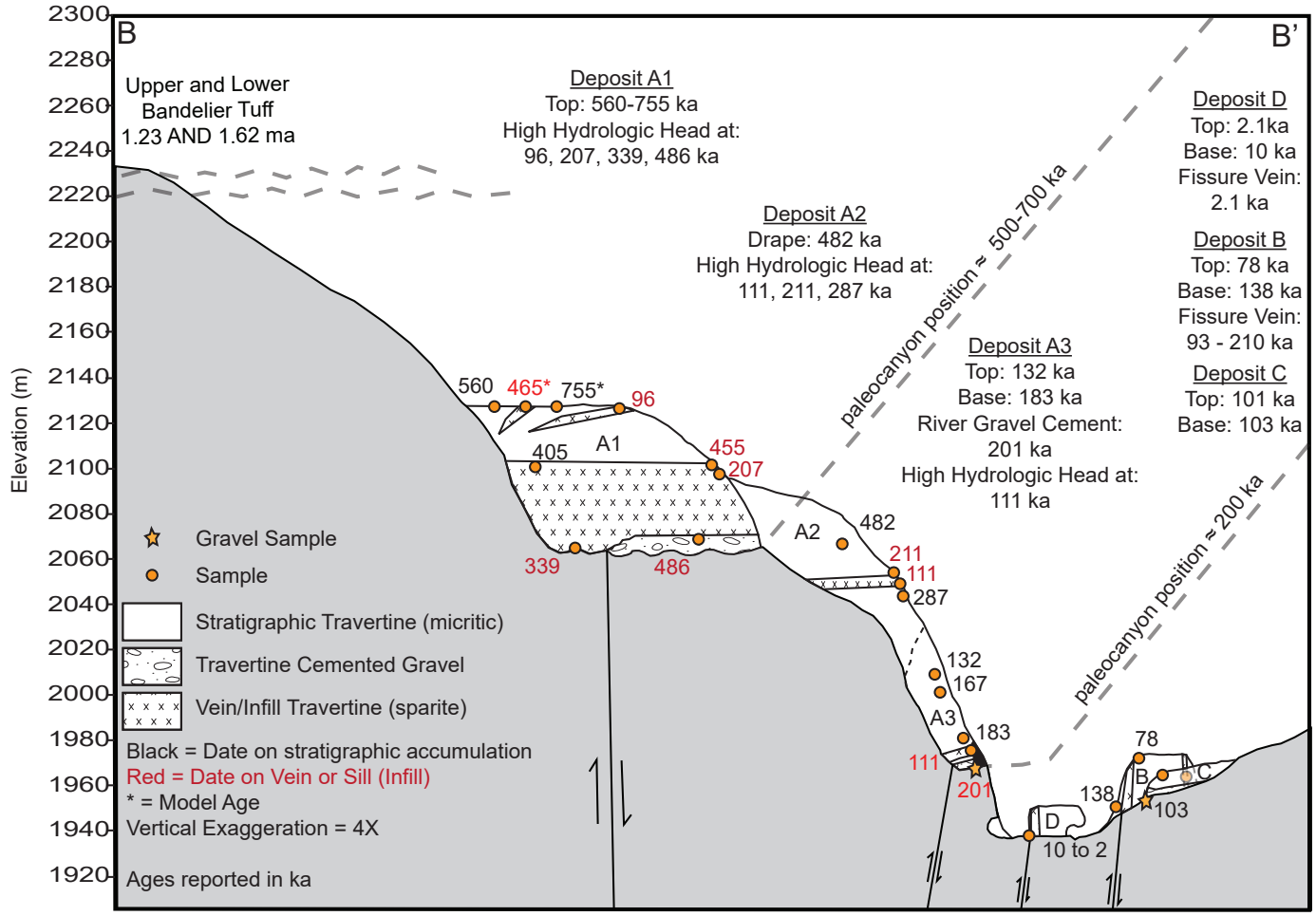

FIGURE 8. Northeast-southwest cross section of San Diego Canyon (A-A' of Fig. 2) showing elevations of gravels, ages of selected travertine samples (from Table 1), and inferred paleocanyon positions at ~500 ka and ~200 ka, as inferred from U-series dating of travertine. All numbers are U-series dates (in ka) and are also listed in Table 1.

TABLE 1. U-series dates from travertines of the Soda Dam system (# = Fig. 3 map #; Age = corrected age in Appendix 1)

#	Deposit	Sample #	Age	(ka)	Remarks	Latitude	Longitude	Elevation
1	A1	LC10-NMSDA-22a	**465***	**± 198**	82 m above Jemez River, horizontal vein of calcite	35.792019	-106.687912	2028
2	A1	LC11-NMSDA-31	**755***	**± 212**	Micritic travertine, top of Deposit A	35.788679	-106.692754	2128
3	A1	LC10-NMSDA-23a	**560**	**± 323**	Stratagraphic travertine just below vein (LC10_ NMSDA_22a)	35.791757	-106.687962	2047
4	A1	AJT11-SDA-51	**486**	**± 125**	Travertine sparite layer within the river gravel layer	35.788659	-106.690961	2071
5	A2	LC10-NMSDA-24	**482**	**± 32**	Drape 70 m below top of platform, 127 m above Jemez River	35.791556	-106.689452	2065
6	A1	LC11-NMSDA-32	**405**	**± 17**	Large sparite cliff, top of vein system	35.786966	-106.694643	2100
7	A1	AJT11-SDA-52	**339**	**± 8**	Travertine sparite vein sitting on Abo formation; base of platform	35.787203	-106.690643	2060
8	A3	LC11-NMSDA-23a	**287**	**± 7**	Stratagraphic travertine just below vein (LC10_ NMSDA_22a)	35.791757	-106.687962	2047
9	A3	LC10-NMSDA-22b	**211**	**± 4**	82 m above Jemez River, horizontal vein of calcite	35.791749	-106.687907	2028
10	B	LC10-SDAM-25B-1	**210**	**± 2**	Lamination in LC10-SdamB-25; Deposit B fissure vein	35.792259	-106.685583	1995
11	A1	LC11-NMSDA-34	**207**	**± 15**	Top of horizontal basal sill in large sparite vein system	35.786966	-106.694643	2100
12	A3	K06-SDAM-2	**201**	**± 2**	Calcite rinds on cobbles right at the bedrock strath	35.792145	-106.687284	1968
13	A3	K06-SDAM-4	**183**	**± 2**	A pour, ~8 m above strath, directly above sill	35.792119	-106.687217	1971
14	A3	LC10-NMSDA-20	**167**	**± 3**	61 m above Jemez River	35.791918	-106.687457	2002
15	B	LC10-SDAM-25B-3	**144**	**± 3**	Lamination in LC10-SdamB-25; Deposit B fissure vein	35.792259	-106.685583	1995
16	B	LC10-NMSDB-15	**137**	**± 1**	11 m above Jemez River, 2 m above exposed base	35.792259	-106.686280	1949
17	B	LC10-SDAM-25B-b	**134**	**± 11**	Lamination in LC10-SdamB-25; Deposit B fissure vein	35.792259	-106.685583	1995
18	A3	LC10-NMSDA-21	**132**	**± 4**	64 m above Jemez River	35.792026	-106.687448	2009
19	B	LC10-SDAM-25B-5	**130**	**± 3**	Lamination in LC10-SdamB-25; Deposit B fissure vein	35.792259	-106.685583	1995
20	B	LC10-SDAM-25B-d	**122**	**± 2**	Lamination in LC10-SdamB-25; Deposit B fissure vein	35.792259	-106.685583	1995
21	B	LC10-SDAM-25B-b	**117**	**± 2**	Lamination in LC10-SdamB-25; Deposit B fissure vein	35.792259	-106.685583	1995
22	A3	K06-SDAM-1	**111**	**± 2**	Calcite sill at the north end of the cave	35.792119	-106.687217	1970
23	A3	LC11-NMSDA-22a	**111**	**± 14**	82 m above Jemez River, horizontal calcite vein in drape	35.792019	-106.687912	2028
24	B	LC10-SDAM-25B-4	**107**	**1.0**	Lamination in LC10-SdamB-25; Deposit B fissure vein	35.792259	-106.685583	1995
25	C	LC10-NMSDC-11	**103**	**0.5**	16.5 m above river, directly above river gravel deposits	35.791854	-106.685530	1954.5
26	C	LC10-NMSDC-13	**101**	**0.5**	23 m above Jemez River, 2 m below top of deposit	35.791938	-106.685377	1961
27	B	LC10-SDAM-25B-a	**98**	**0.8**	Lamination in LC10-SdamB-25; Deposit B fissure vein	35.792259	-106.685583	1995
28	B	LC10-SDAM-25B-c	**96**	**1.0**	Lamination in LC10-SdamB-25; Deposit B fissure vein	35.792259	-106.685583	1995
29	A1	LC11-NMSDA-30	**96**	**8.0**	Top of Deposit A1 spar travertine	35.788679	-106.692754	2128
30	B	LC10-SDAM-25B-2	**92**	**0.5**	Lamination in LC10-SdamB-25; Deposit B fissure vein	35.792259	-106.685583	1995
31	B	LC10-SDB-19	**78**	**1.6**	29.1 m above Jemez River, top of deposit	35.792307	-106.686049	1967
32	D	KLC12-SD-100	**10**	**0.8**	Cross-cutting fissure vein by road; near base	35.791895	-106.686505	1942
33	D	LC11-SDAM-28a	**5.2**	**0.05**	Lamination in LC10-Sdam-28; Soda Dam fissure vein	35.791895	-106.686505	1942
34	D	LC11-SDAM-28c	**4.9**	**0.09**	Lamination in LC10-Sdam-28; Soda Dam fissure vein	35.791895	-106.686505	1942
35	D	LC11-SDAM-28b	**4.6**	**0.05**	Lamination in LC10-Sdam-28; Soda Dam fissure vein	35.791895	-106.686505	1942
36	D	LC11-NMSDA-36	**3.5**	**0.04**	Rind in SD, approximately 3 m in	35.791518	-106.686397	1940
37	D	AJT11-SD-1	**2.1**	**0.03**	Top of cone mound in north-trending fissure	35.791919	-106.686062	1943

All subsample powder weights were between 75 and 400 mg. All ratios are activities, and all uncertainties are absolute 2σ.
All ages are kiloyears before present, where present is 2024 CE.
$\delta^{234}U = (^{234}U/^{238}U_{activity} -1) * 1000$. $\delta^{234}U_m$ = measured $\delta^{234}U$ value, and $\delta^{234}U_i$ = initial $\delta^{234}U$ value.
$\delta^{234}U_m = \delta^{234}U_i * e^{-\lambda 234 t}$, where λ234 is the decay constant for ^{234}U, and t is time in years.
$\delta^{234}U$ age is based on a $\delta^{234}U_i$ value of 600‰ ± 50%, where 600 is the average $\delta^{234}U_i$ value of all ages > 200,000 years old.
* = δ234U model age

model age of 755±212 ka (2 sigma), hence 967 to 543 ka. Minimum ages for the gravel and overlying A1 and A2 platform accumulation are given by several dates: the base of Deposit A1, just above the basal gravel, has a cross cutting calcite spar sill (Fig. 4C) that gives a U-series age of 486±125 ka, similar to a $\delta^{234}U$ model age for a calcite sill near the top of the deposit of 465±198 ka and to a U-series date of 482±32 ka from near the top of the A2 inset drape. These minimum ages range from 486 to 465 ka. Our interpretation of these dates is that the A1 travertine platform developed in and adjacent to the paleoriver on ~500–700 ka gravels and that 400–500 ka was a time of voluminous calcite vein infillings.

As cited above, the inset micritic drape sample in Deposit A2 has an age of 482±32 ka at 70 m below the top of the platform; this was a time when the Deposit A1 platform was still active hydrologically as river incision through the platform was taking place. Another A1 calcite vein sample yielded an age of 405±17 ka, suggesting the platform was saturated with carbonic waters within the 400–500 ka time period. The coarse spar textures of these thick sills is a morphology that is most common in geothermal water deposits (Decker et al., 2016). Additional sparite intrusions infilled the high platform of Deposits A1 and A2 above and near the elevation of the platform base. As shown in Figure 4, high sills yielded ages ranging from 340 to 96 ka, indicating that the spring vents fed by artesian waters continued to be active episodically for several hundred thousand years as the Jemez River progressively incised. We interpret these ages as times of high head in the groundwater system.

In Deposit A3, the lowest part of the inset drape, 201±2 ka travertine formed rinds in river gravels 32 m above the modern river. Stratigraphically coherent ages in this part of the deposit range from 201±2 ka at the base, to a drape of 183±2 just above the base, to 132±4 ka at 64 m above the modern river. A cross-cutting sill, eye-level with the cave near the base of Deposit A3, yielded an age of 111±2 ka.

Deposit B, on the southeast side of the river, was dated to determine both the feeder vein ages and the mound/platform ages. The micritic mound accumulation yielded depositional micrite ages of 137±1 ka near the base and 78±2 ka at the top. Numerous laminations within the ~1-m-wide feeder vein system were dated, yielding ages ranging from 210 to 93 ka (Figs. 6 and 8). The combined data indicate the duration of deposition was 132 ka, from 210 to 78 ka for the Deposit B fissure ridge/mound system, and that it overlapped with development of Deposit A3 from 201 to 111 ka. Deposit C yielded ages of 103±0.5 ka at its base, 16.5 m above the river where travertine overlies colluvium, to 101±0.5 ka at its top, 25 m above the modern river. Its elevation and age overlap with Deposit B, which may have been its source.

Deposit D yielded an oldest age of 10.0±0.8 ka from near its base near road level. Ages from the central fissure vein of Figure 7B ranged from 4.7±0.05 ka to 5.2±0.051 ka. On top of Soda Dam, a small travertine mound at the intersection of two fissure ridges gives a youngest age of 2.1±0.03 ka, and travertine is also being deposited today in several locations.

Figure 9 shows a histogram and age probability plot (from *Isoplot* 3.7 by Ludwig, 2008) that summarize the U-series dates. The age distribution suggests that travertine deposition was episodic. Approximately 77% of the travertine by volume was deposited at or before 500 ka, 14% between 482 and 287 ka, 8% between 183 and 78 ka, and 1% from 10 ka to present. Episodes of high hydrologic head are recorded by cross-cutting calcite veins (many as sills) that have intruded older micritic deposit. The emplacement of sills by artesian waters above the level of the incising Jemez River took place at 95, 110, 210, 340, 455, and 486 ka.

DISCUSSION OF CONTROLS ON TRAVERTINE ACCUMULATIONS AND EPISODIC VARIATIONS IN SPRING DISCHARGE

The Soda Dam travertine system is likely limited by water flux, as opposed to a system that is limited by the flux of external CO_2. Figure 9 shows that dates from the deposits at Soda Dam do not correspond with the timing of volcanic activity in the Valles Caldera. A system limited by the flux of external CO_2 would become diluted during times of high spring discharge and is more probable to produce travertine during climatically dryer conditions (Hancock et al., 1999; Pentecost, 2005; Gilbert et al., 2009; Crossey et al., 2011). However, the Valles Caldera hydrothermal waters have a ready and long-lived source of high P_{CO2}, and faults and fractures allow for circulation of the CO_2-charged waters. Thus, the volume of travertine precipitated is interpreted to be most strongly controlled by spring discharge rate and geometry, influenced by regional wet and dry climate shifts.

Local (caldera lakes) versus regional (wet-dry oscillations) paleohydrology influences on spring discharge are often difficult to separate and were likely complementary to each other during several time intervals. For example, 560 to 520 ka rhyolite dams produced by the San Antonio and South Mountain Dome eruptions may have slowed the Jemez River flow to a trickle and helped amplify artesian head at Soda Dam. The interval of a Valles Caldera lake, represented by core VC-3, may be recorded in the 400–550 ka high-elevation sills in Deposit A1. The present caldera is marshland, with head levels approximately 1000 m above the springs at Soda Dam and paleolake depths of several hundred meters (Goff, 2009) would have episodically increased local hydrologic head. The youngest sample from Deposit A1 is a spar vein sample near the top of 96±8 ka, suggesting high artesian head during interglacial MIS 5 about at the same time Deposits B and C were deposited. Four other spar samples at high elevations in Deposit A1 and A2 yielded ages of 111±14, 207±15, 211±4.6 and 339±8 ka that correspond to MIS 5, 7, and 9/10.

Deposit A3 was deposited from artesian waters that had been pushed up faults and were flowing down a drape deposit toward the Jemez River that was cutting a deeper canyon (Fig. 8). The basal, youngest portion of A3 was apparently eroded by increased flow or a flash flood in the Jemez River to deposit the ~200 ka river gravels that are now 32 m above the modern Jemez River. This deposit was active for at least 52 ka during glacial MIS 6. A cross cutting sill at 110.9±1.5 ka is another

indication of wet periods during interglacial MIS 5.

Deposit B dates indicate travertine accumulation for at least the 130 ka interval that began during interglacial MIS 7 and extended through glacial MIS 6 to the Eemian interglacial (MIS 5; Fig. 9). Its fissure vein system was sampled near the base of the deposit, against country rock, and yielded an oldest date of 210±2 ka, suggesting that subterranean calcite growth began within the Soda Dam fault zone about 70 ka before surface mound accumulation began 138±1 ka.

Soda Dam (Deposit D) began accumulation during the early stages of the current interglacial, apparently later than the pluvial highstands recorded in Lake Estancia at 19.7 and 13.7 ka in central New Mexico (cf. Allen and Anderson, 2000), and it is still actively depositing travertine today. The closely spaced dates from the central fissure vein suggest rapid accumulation around 5 ka.

INCISION HISTORY

The incision history in the Soda Dam area is constrained by U-series dating of travertine associated with preserved gravels at 32 m and 150 m above the modern river. These points are shown on the longitudinal profile of the Jemez River in Figure 10. The lower gravel has travertine coatings around cobbles that yielded an age of 201±2 ka, giving an incision rate of 160 m/Ma. The higher gravel, at the base of Deposit A1, contains 1.2 Ma detrital sanidine and hence is younger than 1.2 Ma (Reed et al., 2024) and is the same age or older than interlayered and overlying travertine. The gravel is intruded by a calcite spar sill of 486±25 ka, which gives a minimum age. Older but still minimum ages are given by imprecise micrite ages from the top of Deposit A1 of 755±212 ka (^{238}U model age) and a U-series age of 568±324 ka. These ages give incision rates of ~200–250 m/Ma, although a rate as low as 155 m/Ma is permitted by the 2σ analytical uncertainty (inset to Fig. 10). The 200–250 m/Ma rate is more compatible with the ~380-m height above river level (ARL) of the base of the 1.62 Ma Otowi Member of the Bandelier Tuff in this area. This gives a long-term average bedrock incision rate of 235 m/Ma since 1.62 Ma, or 309 m/Ma given that little bedrock incision (canyon deepening) occurred

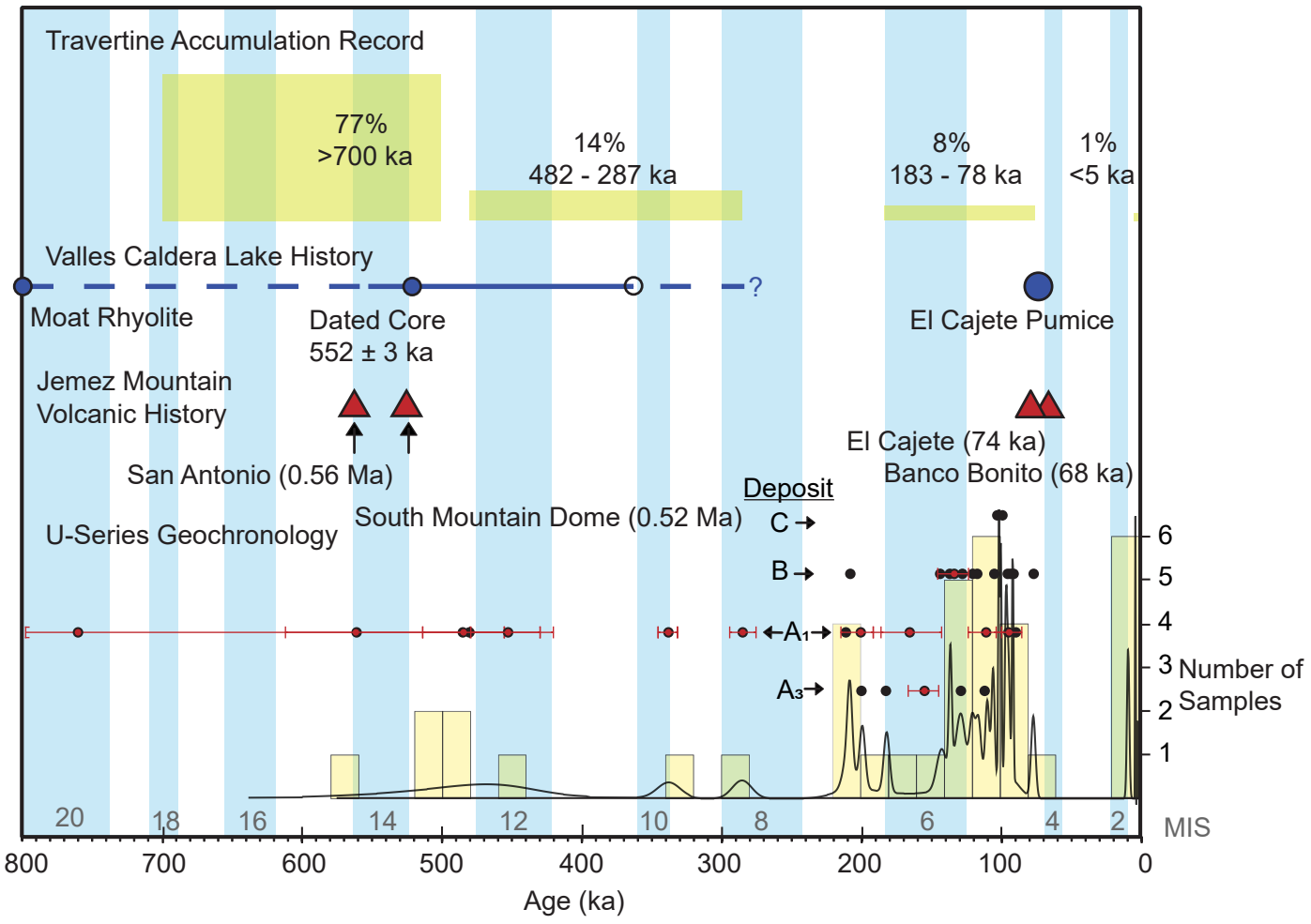

FIGURE 9. Histogram of travertine ages shown in yellow bars. Dated samples (black circles) display error bars in red, except when the error is smaller than the sample point. The age-probability plot displays the sample frequency 2σ error curve in gray. Jemez Mountains volcanic history is from Nashold and Zimmerer (2022); the Valles Caldera lake core record is from Fawcett et al. (2011). This figure suggests that the observed travertine accumulation record was episodic, with the highest volume accumulation (Deposit A) before ~500 ka and subsequent major accumulations about 210 ka (MIS-7), ~120 ka (MIS 5e, 5c, and maybe 5a), and ~10–5 ka at the beginning of the Holocene. Observed travertine episodicity does not correlate well with glacial-interglacial periods or with volcanism and is interpreted to reflect wet times and related lake and high groundwater levels in the Valles Caldera recharge region for the Jemez River.

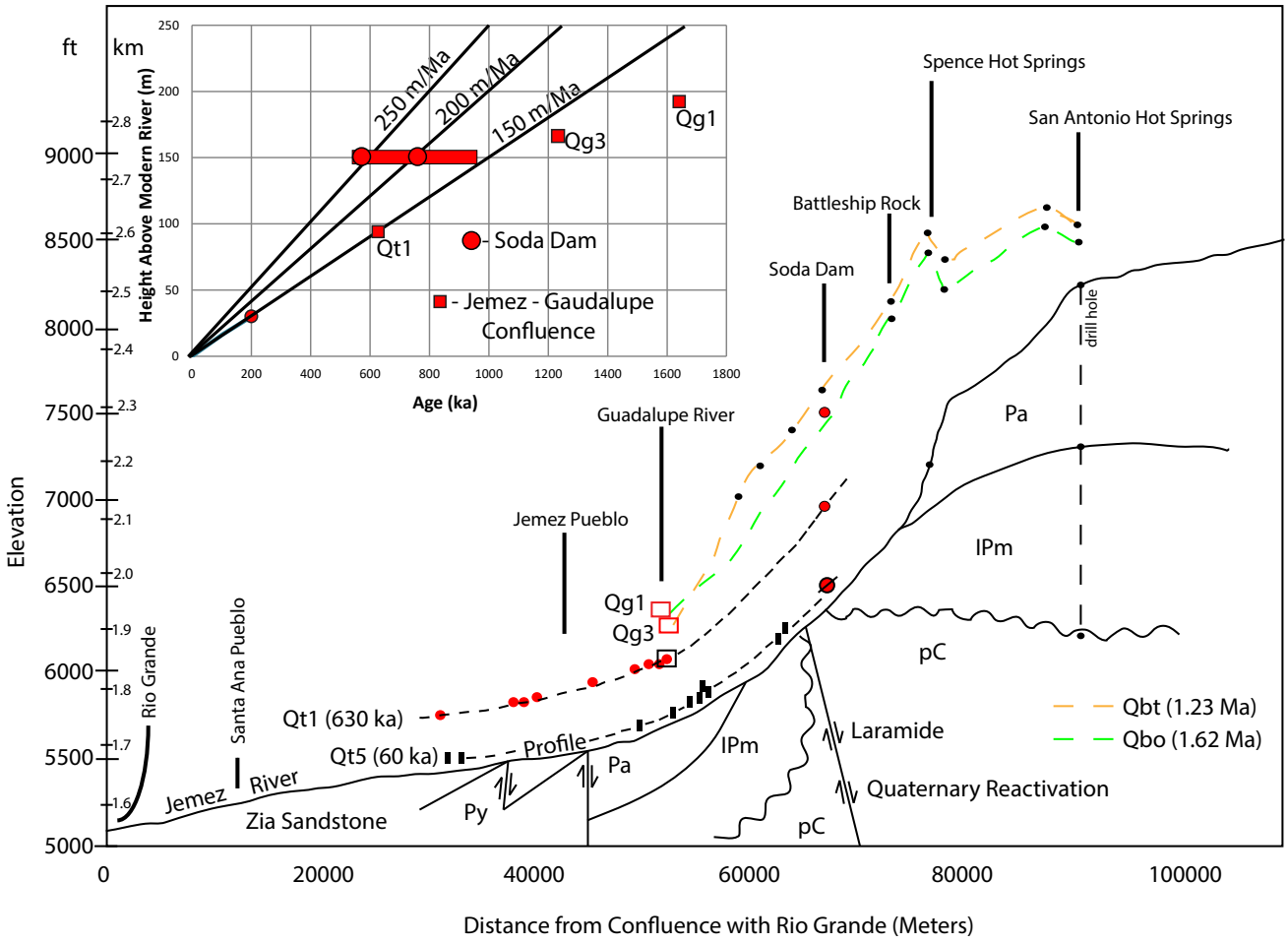

FIGURE 10. Longitudinal profile of the Jemez River from San Antonio hot springs to the confluence with the Rio Grande. The inset graph shows long-term bedrock incision rates of ~143 m/Ma near the confluence of the Jemez and Guadalupe Rivers and probably >200 m/Ma incision rates near Soda Dam.

between the 1.62 and 1.23 Ma Bandelier Tuff eruptions.

These rates contrast with those near the confluence area of the Jemez and Guadalupe Rivers about 15 km downstream. Here, the long-term bedrock incision rate has been steady at 140–150 m/Ma since 1.23 Ma based on gravels coeval with and at the base of the upper Bandelier Tuff (Qg2 and Qg3 of Rogers and Smart, 1996) and based on the 90-m-ARL Qt1 terrace that contains the 0.63 Ma Lava Creek B ash that gives 143 m/Ma. Figure 10 suggests that the 150-m-ARL Soda Dam gravels may correlate with the thick and laterally extensive downstream Lava Creek B terrace. If so, this would give an average bedrock incision rate of 238 m/Ma at Soda Dam over the past 630 ka, similar to 235 m/Ma since 1.62 Ma. Improved dating on the high gravels is needed, but our present interpretation is that average long-term bedrock incision rates at Soda Dam are higher (200–250 m/Ma) than at the Guadalupe River confluence (140–150 m/Ma) due 50–100 m/Ma Quaternary slip on the Jemez fault system (Reed et al., 2024). This new geochronology is not compatible with the terrace correlation shown by Frankel and Pazzaglia (2006, fig. 8), who correlated the 630 ka terrace near the Jemez-Guadalupe confluence with our newly dated 210 ka terrace at Soda Dam. This change is important because it weakens their conclusion of upstream-converging terraces and changes it to upstream- diverging, which is more compatible with fault-related headwater uplift (Reed et al., 2024) rather than downstream base level fall (Frankel and Pazzaglia, 2006).

SUMMARY AND CONCLUSIONS

Periods of travertine accumulation were episodic at Soda Dam, occurring at approximately 500, 200,140–90, and 10–0 ka, with records of high artesian head at approximately 95, 110, 210, 340, 455, and 486 ka. Development of the Valle San Antonio and Valle Grande paleolakes at ~520 ka were likely the cause of the high hydrologic head and the accumulation of the large-volume Deposit A1 that developed in the paleo-Jemez River ~700–500 ka. This episodicity indicates that the unique hydrologic and geomorphic setting of Soda Dam involves: (1) long-lived fault-related spring vents for hydrothermal waters, (2) episodic high heads suggesting wet intervals and the presence of caldera lakes, and (3) river water that was draining caldera lakes and reincising San Diego Canyon.

Travertine deposition reflects a variety of influences, but the nature of the Jemez magmatic system suggests there is generally enough CO_2 to deposit travertine, that faults have acted as

conduits for ascent and transport of magmatic volatiles, and that mixing of endogenic and meteoric waters is responsible for the wide variation in modern water and gas chemistry and for determining travertine geochemistry.

Tectonic influences include travertine deposition along faults, different rates of canyon incision across active Quaternary faults, a persistent upgradient geothermal field, and pulses of caldera magmatism that influenced the formation and demise of paleolakes. The combined data are significant regionally in providing one of the best records of episodic hydrothermal groundwater discharge, as affected by both high-elevation caldera paleolakes and wet climate intervals in one of the most volcanically active regions and most important geothermal systems of the southwestern United States.

ACKNOWLEDGMENTS

Funding for this project came primarily from NSF-EAR-0838575 to Crossey and Karlstrom. Additional support was from the NM Epscor RII4: Energize new Mexico (NSF #1301346). April Tafoya Jean's master's thesis was supported by NSF Louis Stokes for Minority Participation Bridge to the Doctorate Fellowship through #NSF/EHR 1026412 and NSF EAR/0838575 (to Crossey). The NSF 326902 instrument grant (to Asmerom) also provided support. We thank Dr. Peter Fawcett; Dr. Fraser Goff and the various researchers associated with the Valles Caldera projects; and Alexandra Preiswich, Rebecca Wacker, Ryan Crow, Zachary LaPointe, Brandi Cron, Andy Jochems, Chris Cox, Miela Kolomaznik, and Kyle Paffett for helpful discussions. We thank Matt Heizler, Shari Kelley, and Jayne Aubele for reviews that improved the paper.

REFERENCES

Allen, B.D., and Anderson, R.Y., 2000, A continuous, high-resolution record of late Pleistocene climate variability from the Estancia basin, New Mexico: Geological Society of America Bulletin, v. 112, p. 1444–1458.

Asmerom, Y., Polyak, V., Schwieters, J., and Bouman, C., 2006, Routine high-precision U–Th isotope analyses for paleoclimate chronology: Geochimica et Cosmochimica Acta, v. 70, no. 18, https://doi.org/10.1016/j.gca.2006.06.061

Ballentine, C.J. and Burnard, P.G., 2002, Production, release and transport of noble gases in the continental crust, *in* Porcelli, D., Ballentine, C.J., and Weiler, R., eds., Reviews in Mineralogy and Geochemistry: Noble Gases in Geochemistry and Cosmochemistry, v. 47: Washington, D.C., Mineralogical Society of America, p. 481–538.

Ballentine, C.J., Burnard, P.G., Marty, B., 2002, Tracing fluid origin, transport and interaction in the crust, *in* Porcelli, D., Ballentine, C.J., and Wieler, R., eds., Reviews in Mineralogy and Geochemistry: Noble Gases in Geochemistry and Cosmochemistry, v. 47: Washington, D.C., Mineralogical Society of America, p. 539–614, https://doi.org/10.2138/rmg.2002.47.13

Cheng, H., et al., 2013, Improvements in ^{230}Th dating, ^{230}Th and ^{234}U half-life values, and U–Th isotopic measurements by multi-collector inductively coupled plasma mass spectrometry: Earth and Planetary Science Letters, v. 371, p. 82–91, https://doi.org/10.1016/j.epsl.2013.04.006

Crossey, L.J., Fischer, T.P., Patchett, P.J., Karlstrom, K.E., Hilton, D.R., Newell, D.L., Huntoon, P., Reynolds, A.C., and de Leeuw, G.A.M., 2006, Dissected hydrologic system at the Grand Canyon: Interaction between deeply derived fluids and plateau aquifer waters in modern springs and travertine: Geology, v. 34, p. 25–28, https://doi.org/10.1130/G22057.1

Crossey, L.J., Karlstrom, K.E., Springer, A.E., Newell, D., Hilton, D.R., and Fischer, T., 2009, Degassing of mantle-derived CO2 and He from springs in the southern Colorado Plateau region: Neotectonic connections and implications for groundwater systems: Geological Society of America Bulletin, v. 121, p. 1034–1053, https://doi.org/10.1130/B26394.1

Crossey, LJ., Karlstrom, K.E., Newell, D., Kooser, A., and Tafoya, A., 2011, The La Madera Travertines, Rio Ojo Caliente, northern New Mexico: Investigating the linked system of CO2-rich springs and travertines as neotectonic and paleoclimate indicators, in Koning, D.J., Karlstrom, K.E., Kelley, S.A., Lueth, V.W., and Aby, S.B., eds., Geology of the Tusas Mountains - Ojo Caliente: New Mexico Geological Society Guidebook 62, p. 301–316.

Decker, D.D., Polyak, V.J., and Asmerom, Y., 2016, Depth and timing of calcite spar and 'spar cave' genesis: Implications for landscape evolution studies, *in* Feinberg, J., Gao, Y., and Alexander, E.C., Jr., eds., Caves and Karst Across Time: Geological Society of America Special Publication 516, p.103–111.

Embid, E.H., 2009, U-Series dating, geochemistry, and geomorphic studies of travertines and springs of the Springerville area, East-Central Arizona, and tectonic implications [M.S. thesis]: Albuquerque, University of New Mexico, 103 p.

Fawcett, P.J., et al., 2011, Extended megadroughts in the southwestern United States during Pleistocene interglacials: Nature, v. 470, p. 518–521, https://doi.org/10.1038/nature09839

Frankel, K.L., and Pazzaglia, F.J., 2006, Mountain fronts, base-level fall, and landscape evolution: Insights from the southern Rocky Mountains, *in* Willett, S.D., Hovius, N., Brandon, M.T., and Fisher, D.M. eds., Tectonics, Climate, and Landscape Evolution: Geological Society of America, v. 398, https://doi.org/10.1130/2006.2398(26)

Gilbert, R.O., Taberner, C., Saez, A., Giralt, S., Alonso, R.N., Edwards, R.L., and Pueyo, J.J., 2009, Igneous origin of CO_2 in ancient and recent hot-spring waters and travertines from the northern Argentinean Andes: Journal of Sedimentary Research, v. 79, p. 554–567, https://doi.org/10.2110/jsr.2009.061

Goff, F., 2002, Gas geochemistry of the Valles Caldera region, New Mexico and comparisons with gases at Yellowstone, Long Valley and other geothermal systems: Journal of Volcanology and Geothermal Research, v. 116, no. 3–4, p. 299–323, https://doi.org/10.1016/S0377-0273(02)00222-6

Goff, F., 2009, Valles Caldera: A Geologic History: Albuquerque, University of New Mexico Press, 128 p.

Goff, F., and Gardner, J.N., 1994, Evolution of a mineralized geothermal system, Valles Caldera, New Mexico: Economic Geology, v. 89, p. 1803–1832, https://doi.org/10.2113/gsecongeo.89.8.1803

Goff, F., and Janik, C.J., 2002, Gas geochemistry of the Valles Caldera region, New Mexico and comparisons with gases at Yellowstone, Long Valley and other geothermal systems: Journal of Volcanology and Geothermal Research, v. 116, p. 299–323, https://doi.org/10.1016/S0377-0273(02)00222-6

Goff, F. and Shevenell, L., 1987, Travertine deposits of Soda Dam, New Mexico, and their implications for the age and evolution of the Valles Caldera hydrothermal system: Geological Society of America Bulletin, v. 99, p. 292–302, https://doi.org/10.1130/0016-7606(1987)99<292:TDOSD-N>2.0.CO;2

Goff, F., Shevenell, L., Gardner, J.N., Vuataz, F.D., and Grigsby, C.O., 1988, The hydrothermal outflow plume of Valles Caldera, New Mexico, and a comparison with other outflow plumes: Journal Geophysical Research, v. 93, p. 6041–6058, https://doi.org/10.1029/JB093iB06p06041

Hancock, P.L., Chalmers, R.M.L., Altunel, E., and Çakir, Z., 1999, Travertonics: Using travertines in active fault studies: Journal of Structural Geology, v. 21, p. 903–916, https://doi.org/10.1016/S0191-8141(99)00061-9

Heinken, G., Goff, F., Gardner, J.N., and Baldridge, W.S., 1990, The Valles/Toledo Caldera complex, Jemez volcanic field, New Mexico: Annual Reviews of Earth and Planetary Sciences, v. 18, p. 27–53, https://doi.org/10.1146/annurev.earth.18.1.27

Jean, A., 2012, Uranium-series dating of travertine from Soda Dam, New Mexico: A Quaternary record of episodic, climate-driven spring discharge and river incision in the Jemez Mountains hydrothermal system [unpublished M.S. thesis]: Albuquerque, University of New Mexico, 118 p.

Karlstrom, K.E., Crow, R., Crossey, L.J., Coblentz, D., Van Wijk, J.W., 2008, Model for tectonically driven incision of the younger than 6 Ma Grand Canyon: Geology, v. 36, no. 11, p. 835–838, https://doi.org/10.1130/G25032A.1

Kelley, S., Kempter, K.A., Goff, F., Rampey, M., Osburn, B., and Ferguson, C.A., 2003, Preliminary geologic map of the Jemez Springs 7.5-minute quadrangle: New Mexico Bureau of Geology and Mineral Resources Open-File Geologic Map 73, scale 1:24,000, https://doi.org/10.58799/OF-GM-73

Lisiecki, L.E., and Raymo, M.E., 2005, A Pliocene-Pleistocene stack of 57 globally distributed benthic $\delta^{18}O$ records: Paleoceanography, v. 20, p. 1003.

Ludwig, K.R., 2008, Isoplot/Ex 3.7 Beta: A Geochronological Toolkit for Microsoft Excel: Berkeley, CA, Berkeley Geochronology Center.

McGibbon, C., Crossey, L.C., Karlstrom, K.E., and Grulke, T., 2018, Carbonic springs as distal manifestations of geothermal systems, highlighting the importance of fault pathways and hydrochemical mixing: Example from the Jemez Mounrains, New Mexico: Applied Geochemistry, v. 98, p. 45–57, https://doi.org/10.1016/j.apgeochem.2018.08.015

Moats, W., 2004, Geology of the Soda Dam travertine deposits, Sandoval County, New Mexico: New Mexico Geological Society Spring Meeting Abstracts, https://doi.org/10.56577/SM-2004.711

Nasholds M.W.M., and Zimmerer, M.J., 2022, High-precision $^{40}Ar/^{39}Ar$ geochronology and volumetric investigation of volcanism and resurgence following eruption of the Tshirege Member, Bandelier Tuff, at the Valles caldera: Journal of Volcanology and Geothermal Research, v. 431, 107624, https://doi.org/10.1016/j.jvolgeores.2022.107624

Newell, D.L., Crossey, L.J., Karlstrom, K.E., and Fischer, T.P., 2005, Continental scale links between the mantle and groundwater systems of the western United States: Evidence from the travertine springs and regional He isotope data: GSA Today, v. 15, no. 12, p. 4–10, https://doi.org/10.1130/1052-5173(2005)015<4:CSLBTM>2.0.CO;2

Pederson, J.L., Anders, M.D., Ritenhour, T.M., Sharp, W.D., Gosse, J.C., and Karlstrom, K.E., 2006, Using fill terraces to understand incision rates and evolution of the Colorado River in eastern Grand Canyon, Arizona: Journal of Geophysical Research (Earth Surface), v. 111, F02003, https://doi.org/10.1029/2004JF000201

Pentecost, A., 2005, Travertine: Berlin, Springer.

Priewisch, A., Karlstrom, K.E., and Crossey, L.J., 2013, U-series ages and morphology of a Quaternary large-volume travertine deposit at Mesa del Oro, NM, Implications for paleohydrology, paleoclimate, and neotectonic processes, *in* Ziegler, K., Timmons, J.M., Timmons, S., and Semken, S., eds., Geology of Route 66 Region: Flagstaff to Grants: New Mexico Geological Society Guidebook 64, p. 229–237, https://doi.org/10.56577/FFC-64.229

Reed, C., Karlstrom, K.E., Rodriguez, B., Iverson, N., Heizler, M., Rose-Coss, D., Crossey, L.C., Cox, C., Jean, A.J., Polyak, V., and Asmerom, Y., 2024, Differential river incision due to Quaternary faulting on Río Salado-Jemez system at the million-year timescale, *in* Karlstrom, K.E., Koning, D.J., Lucas, S.G., Iverson, N.A., Crumpler, L.S., Aubele, J.C., Blake, J.M., Goff, F., and Kelley, S.A., eds., Geology of the Nacimiento Mountains and Río Puerco Valley: New Mexico Geological Society Guidebook 74 (this volume), p. 237–256.

Rogers, J.B. and Smartt, R.A., 1996, Climatic influences on Quaternary alluvial stratigraphy and terrace formation in the Jemez River valley, New Mexico, *in* Goff, F., Kues, B.S., Rogers, M.A., McFadden, L.D., and Gardner, J.N., eds., Jemez Mountains Region: New Mexico Geological Society Guidebook 47 New Mexico Geological Society Guidebook 47, https://doi.org/10.56577/FFC-47.347

Szabo, B. J., 1990, Ages of travertine deposits in eastern Grand Canyon National Park, Arizona: Quaternary Research, v. 34, p. 24–32, https://doi.org/10.1016/0033-5894(90)90070-2

Vuataz, F.D., and Goff, F., 1986, Isotope geochemistry of thermal and nonthermal waters in the Valles Caldera, Jemez Mountains, Northern New Mexico: Journal of Geophysical Research, v. 91, p. 1835–1853.

Wilgus, J., Schmandt, B., Maguire, R., Jiang, C., Chaput, J., 2023, Shear velocity evidence of upper crustal magma storage beneath Valles Caldera: Geophysical Research Letters, v. 50, no. 5, e2022GL101520, https://doi.org/10.1029/2022GL101520

Appendices can be found at https://nmgs.nmt.edu/repository/index.cfml?rid=2024004